Journal of Visualization, Vol. 6, No. 2 (2003) 185-193

Dependence of Aerodynamic Characteristics and Flow Pattern on Surface Structure of a Baseball

Aoki, K.*[1], Kinoshita, Y.*[2], Nagase, J.*[3] and Nakayama, Y.*[4]

*1 Department of Mechanical Engineering, Tokai University, School of Engineering, 1117 Kitakaname, Hiratsuka, Kanagawa 259-1292, Japan.
*2 Graduate student, Course of Mechanical Engineering, Graduate School of Engineering, Tokai University.
*3 NAGASE KENKO Co. Ltd., 2-36-10 Sumida, Sumida-ku, Tokyo 131-8520, Japan.
*4 Future Technology Research Institute, 3-56-2 Higashi-Oizumi, Nerima-ku, Tokyo 178-0063, Japan.

Received 12 June 2002
Revised 9 September 2002

Abstract : In this report, the aerodynamic characteristics, such as lift and drag, of an official rubber baseball are studied experimentally by comparing the characteristics of a sphere having a smooth surface and those of spheres having different surface structures. In addition, the flow velocity distribution is measured quantitatively using the spark tracing method. From the obtained results, the flow patterns for these baseballs and the flow mechanism around a sphere have been clarified.

Keywords : Seam, Dimple, Drag coefficient, Lift coefficient, Spin rate

1. Introduction

In the game of baseball, the technique of throwing a “braking ball” is important. There have been several reports showing the aerodynamic characteristics associated with the “knuckle ball” and the “forkball” [Mizota et al., 1995]. In Japanese primary and junior-high schools, rubber balls are widely used in local league baseball games instead of the traditional hard baseball. The surface of the rubber ball has linear trapezoidal projections that are similar to the seams of a normal baseball, and the surface is covered by elliptical and circular dimples similar to those of a golf ball. The dimples on a golf ball have the effect of decreasing drag and increasing flight distance. However, the dimples on a rubber ball are due to the industrial design, and their effect has not been examined from the viewpoint of aerodynamic characteristics. The aim of the present research is to investigate the aerodynamic characteristics associated with the surface design of rubber baseballs.

In this report, the experimental results are presented in order to reveal the aerodynamic characteristics of the official rubber ball, including lift and drag, and compares these characteristics to the aerodynamic characteristics of a smooth ball and to balls having different surface shapes. The results include the influence of seams and dimples on the aerodynamic characteristics of rotating test balls in flight with the spin rate a ($=V/U$, V : peripheral velocity of ball, U : flow

velocity); and the flow velocity distribution is measured quantitatively using the spark tracing method.

2. Experimental Apparatus and Method

2.1 Test balls

Five different types of balls, shown in Fig. 1, were tested, and their key specifications are listed in Table. 1.

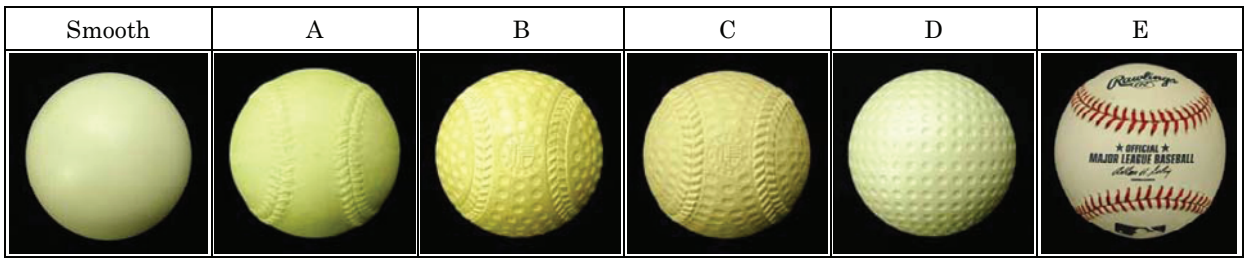

Fig. 1. Test balls.

Table 1. Specification of the test ball.

Type	D [mm]	Seam	Dimple	Number of Dimples
Smooth	80.00	—	—	—
A	72.20	○	—	—
B	71.16	○	○	304
C	71.14	○	○	324
D	71.20	—	○	462
E	73.00	○	—	—

2.2 Experimental apparatus and data processing

A circulating wind tunnel having an exit nozzle area of 700 × 700 mm^2 was used in the present experiment. As shown in Fig. 2, a rectangular frame of area 800 × 800 mm^2 was placed on a strut-type six-component balance at a position 100 mm downstream from the inlet of the wind tunnel. A test ball is fixed at the center of the test section using string which provides tension at both ends of the ball. The drag and lift acting on the test ball are measured using a six-component measuring device. The diameter of the piano wire, which yields negligible interference effect on the drag measurement, is 3/32 inch [= 2.38 mm]. The number of rotations of the test ball is adjusted by adjusting the voltage of a motor connected to the wire.

In the experiment, the drag and lift are measured for wind tunnel velocities ranging from 5 to 35 m/s at 5 m/s intervals. The Reynolds numbers for these flow velocities range from 2.3 × 10^4 to 1.6 × 10^5. Measurements of the ball having the seam on the surface was made by changing θ from 0°

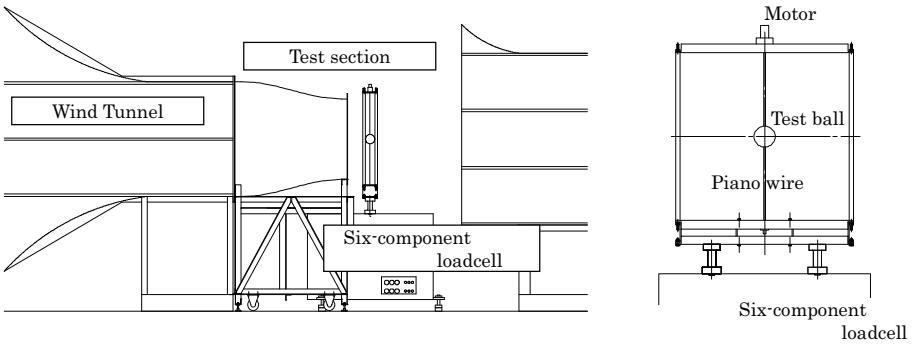

Fig. 2. Experimental apparatus.

to 90° at 10° intervals in the clockwise direction from the state shown in Fig. 3, where θ is the angle of the ball relative to the incoming flow direction. The flow velocity distribution is measured quantitatively using the spark tracing method. In this method, a series of pulses is supplied at a constant interval (pulse interval: 250 μs) by a high-voltage, high-frequency pulse generator, and spark trains are recorded on photographic film. Measurements are made by changing the rotation rate of the test balls from 1000 rpm to 3500 rpm at 250 rpm intervals.

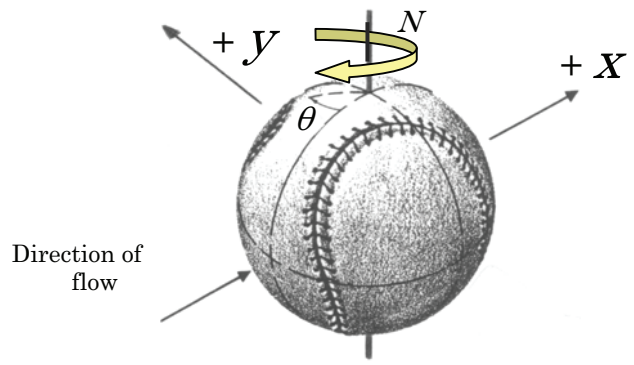

Fig. 3. Coordinate system for measuring air flow characteristics.

From the measured values, the drag and lift coefficients C_D and C_L are calculated based on the following equations.

$$D = C_D \cdot A \cdot \rho \cdot \frac{U^2}{2} \qquad [\mathrm{N}] \tag{1}$$

$$L = C_L \cdot A \cdot \rho \cdot \frac{U^2}{2} \qquad [\mathrm{N}] \tag{2}$$

A : spherical projection area, ρ : density, U : uniform velocity

3. Experimental Results and Discussion

3.1 Drag coefficient under the non-rotation condition

Figure 4 shows the drag coefficient of each sample ball at the ball direction $\theta = 0°$. Although, in general, the drag coefficient has a critical Reynolds number of around 3.5×10^5 for the smooth ball,

the critical region of test balls A through E moves toward the region of lower Reynolds number. Therefore, the effect of the seam on the rubber ball is to decrease drag in a similar way as the effect of dimples on golf balls [Berman and Harvey, 1976]. Furthermore, the drag coefficient differs depending on the test ball. The drag coefficient for test ball D at the critical Reynolds number is lower than that for the test ball A. For the case of test balls B and C with seams and dimples, respectively, the critical Reynolds number is even lower than that of test ball A. Comparing test balls B and C, the critical Reynolds number is lower and the minimum drag coefficient is higher for test ball C.

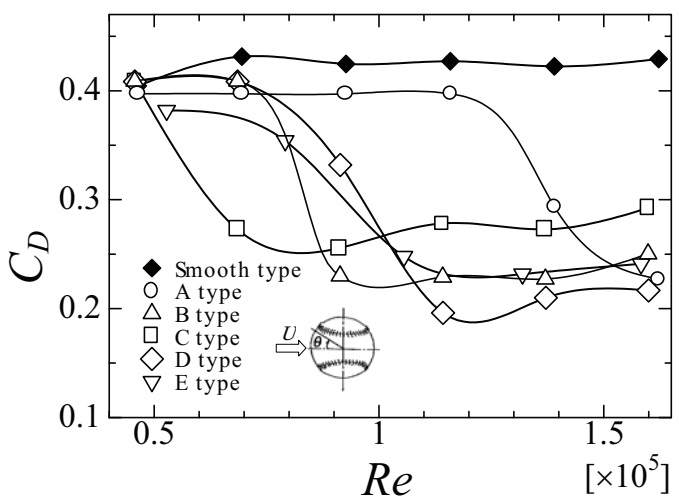

Fig. 4. Drag coefficient for $\theta = 0°$.

Figure 5 shows the drag coefficients of test balls A, B, and C at different ball angles. From the figures, it can be seen that the drag coefficients in the critical region are dependent on the ball angle θ. Drag coefficient increases as θ increases from $\theta = 0°$, and becomes maximum at about 40°, followed by a gradual decrease.

3.2 Spark tracing method

Figure 6 shows the geometry of the spark tracing method set-up. The photographs taken using this method are shown in Fig. 7 (a)~(c) for test ball A and in Fig. 8 (a)~(c) for test ball C corresponding respectively to $Re = 0.5\times10^5$, 0.9×10^5, and 1.4×10^5. From these figures, the drag coefficients of test balls A and C at $Re = 0.5\times10^5$ are found to be in the subcritical region. So, the positions of the separation points in Figs. 7 (a) and 8 (a) are almost equal at $\theta = \pm85°$, and the wake region formed downstream of the ball are virtually identical.

The drag coefficient at $Re = 0.9\times10^5$ indicates that test ball A is in the subcritical region, but test ball C moves into the critical region. So, the position of the separation points in Fig. 7(b) is about $\theta = \pm85°$, but that of Fig. 8(b) is at about $\theta = \pm120°$.

The drag coefficients at $Re = 1.4\times10^5$ indicate that both test balls A and C are in the supercritical region. So, the position of the separation points in Figs. 7(c) and 8(c) are at about $\theta = \pm120°$.

3.3 Relationship between lift and rotating angle

Figure 9 illustrates the force acting on test balls A, B, C and E in the y-direction in terms of

the ball angles. According to this figure, the force changes periodically in four cycles during 360° rotation regardless of flow velocity. The lift becomes maximum at θ=20~40°, and at θ=40~60°, the lift takes a negative value. The lift of test balls B and C do not change significantly as the flow velocity increases; however, the lift of test balls A and E increase at Re=1.4×10^5.

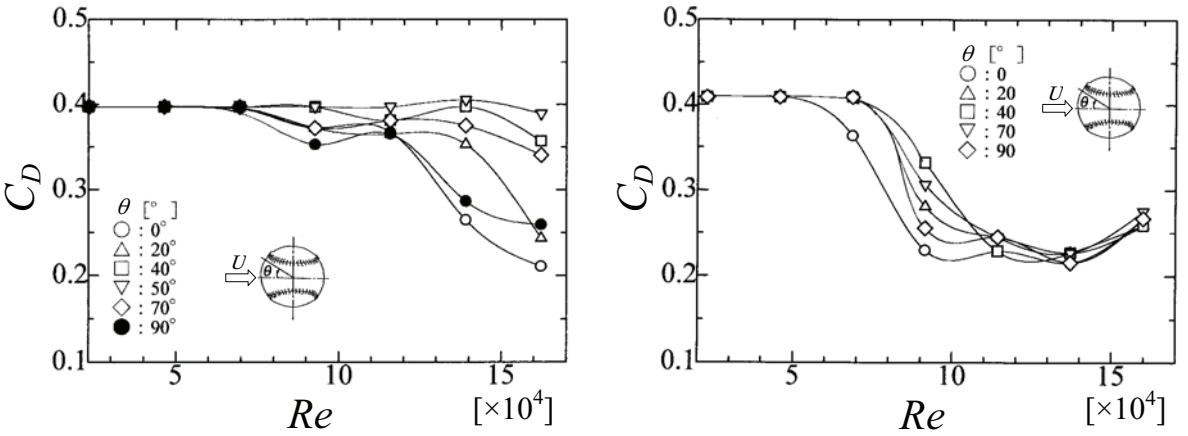

(a) test ball A

(b) test ball B

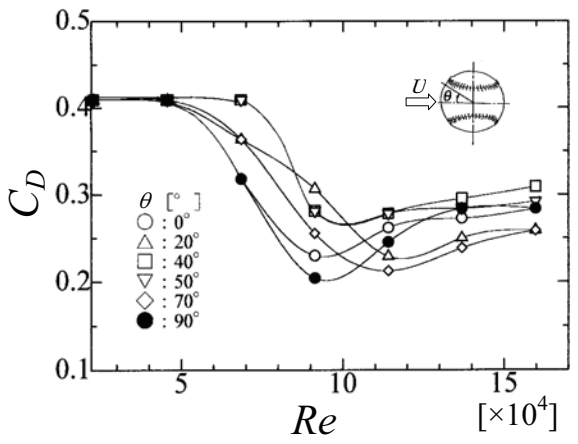

(c) test ball C

Fig. 5. Drag coefficient for different ball angles.

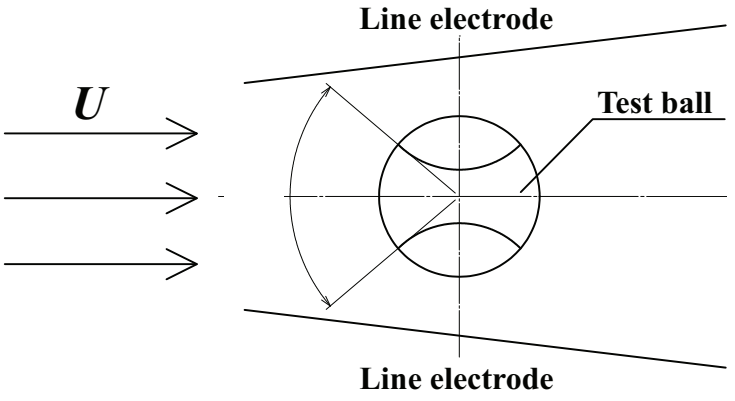

Fig. 6. Geometry of the spark tracing method (Top view).

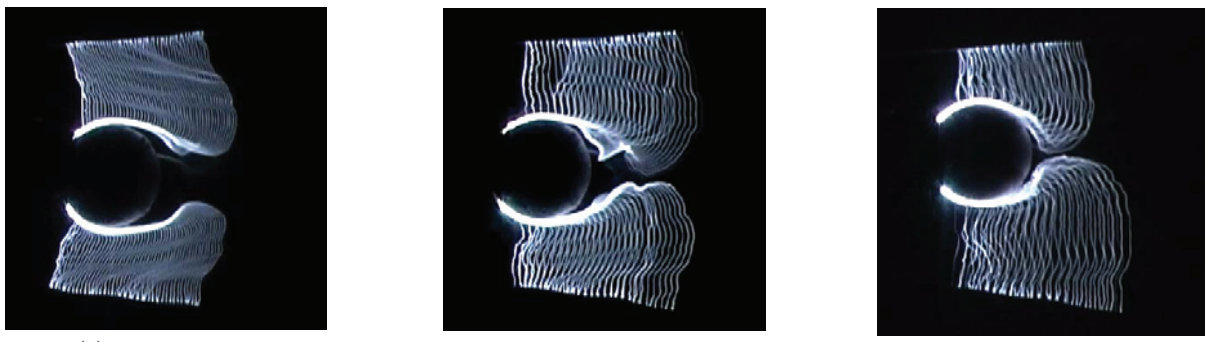

(a) $Re = 0.5\times10^5$ (b) $Re = 0.9\times10^5$ (c) $Re = 1.4\times10^5$

Fig. 7. Visualization of flows around a ball (test ball A).

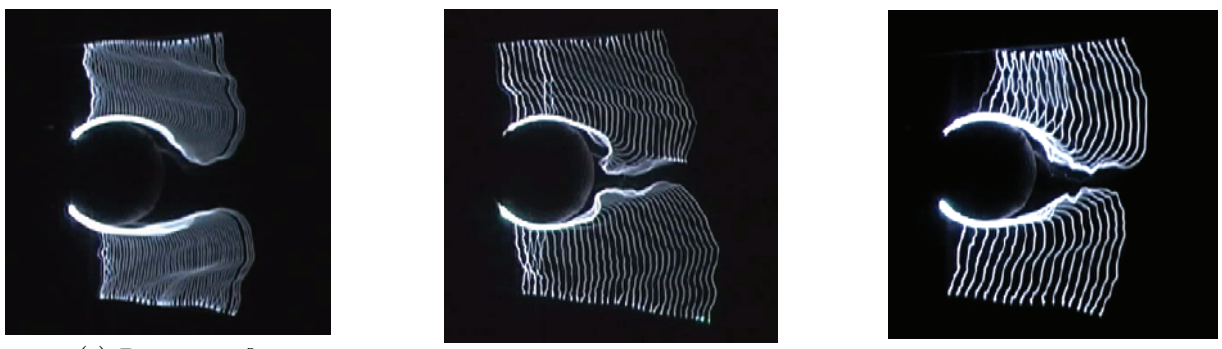

(a) $Re = 0.5\times10^5$ (b) $Re = 0.9\times10^5$ (c) $Re = 1.4\times10^5$

Fig. 8. Visualization of flows around a ball (test ball C).

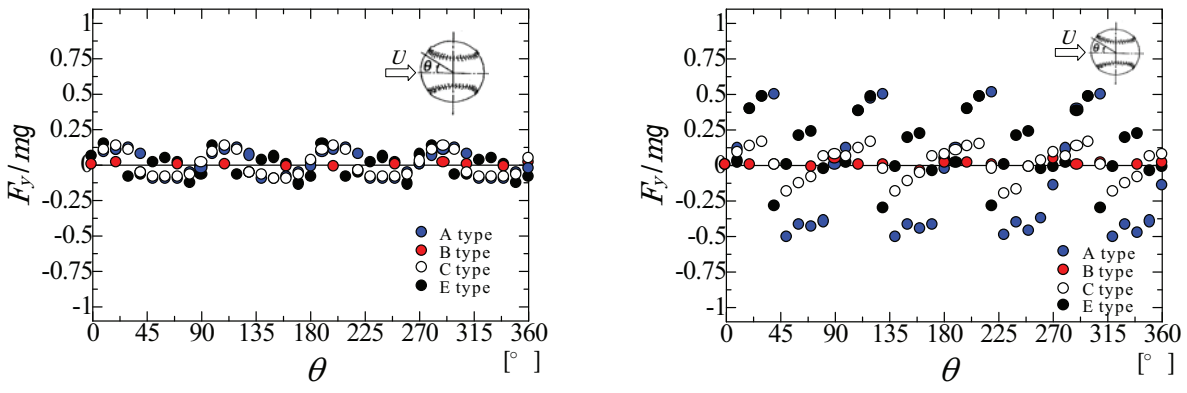

(a) Re=0.7×10^5 (b) Re=1.4×10^5

Fig. 9. Force in the y-direction for various test balls.

3.4 Flying Characteristics of rotating test ball

Figure 10 shows the change in C_D and C_L as a function of spin rate a (=V/U, V: peripheral velocity of test ball, U: flow velocity) for a smooth test ball. In this range of Reynolds numbers, the lift is in the negative direction at a=0.1~0.6. Moreover, the lift has shifted to the positive direction at a>0.6. The region of Re and a, in which the negative lift is generated is shown in Fig. 11. The region of negative lift generation in Taneda's experiments [Taneda, S.,1957] is shown as a dark

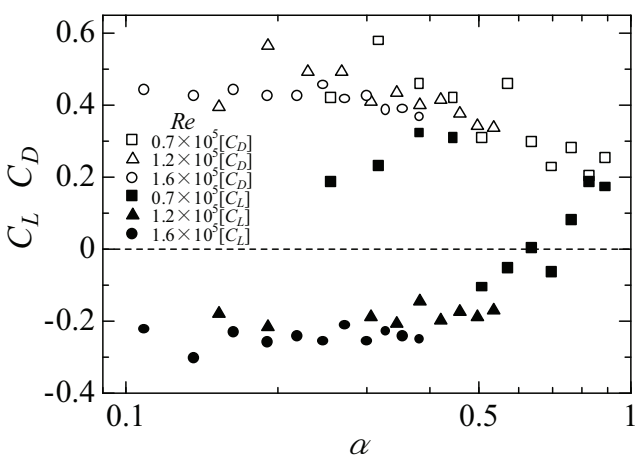

Fig. 10. Lift and drag coefficients vs. spin rate α (smooth test ball).

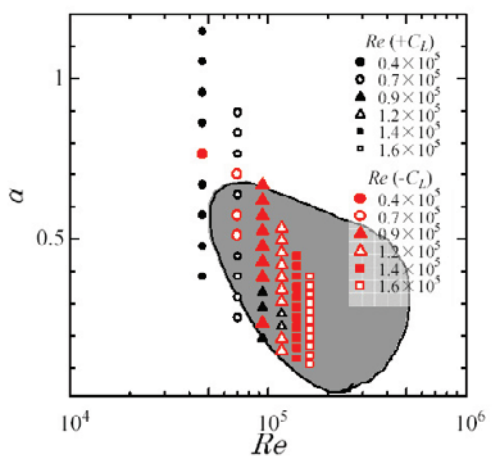

Fig. 11. Region of negative Magnus force in the (Re, α) plane.

hatched part in Fig. 11. As shown in this figure, the present experimental results agree with Taneda's experimental results. This phenomenon is known as the "negative Magnus effect". In these regions, the flow of the increasing speed side becomes laminar and the separation point shifts upstream. As against this, the flow of the decreasing speed side becomes turbulent and the separation point shifts downstream. Therefore, a reverse force is considered to act on the sphere. Generally, the C_D of the sphere without rotation decreases as Re increases. When the sphere rotates, C_D decreases with increasing α at the same Re. In Fig. 10, C_D begins to decrease from α=0.3~0.4, and, conversely, C_L begins to increase from α=0.3~0.4. Both values become similar at α=1. C_D and C_L of the rotating test ball at Re=1.6×10^5 are shown in Figs. 12 and 13, respectively. Comparison of C_D between different balls shows the following: the values of C_D for the smooth test ball are, on average, largest among the test balls, C_D of the smooth test ball decreases as α increases, and becomes smaller than those for test balls A through E in the region α>0.37. The average number of rotations of the ball when thrown by a pitcher in a game is N=2500 rpm or less, corresponding to α=0.27 or less. The drag coefficient of test ball D with only dimples has the lowest value, and the coefficient of type E with only seam has maximum value. From this result, it becomes clear that dimples on the surface of a ball decrease drag more effectively than does the seam.

Next, test ball C, which is the rubber ball generally used in baseball games, is compared with test ball E, which is used in the major leagues. As shown in Fig. 4, when the test ball is not rotating, C_D for test ball C is lower than for other test balls at Re=0.7×10^5. However, when Re becomes over 1.2×10^5, the C_D of test ball C and the C_D of test ball E have similar values. If rotation is given to the ball, the drag coefficient of test ball C becomes slightly smaller than that of test ball E, as shown in Fig. 12. Therefore, the dimples on the surface of the baseball also decrease drag. When a pitcher throws a ball, a rubber ball has a drag that is lower than that of a traditional hard ball. Moreover, C_D of test ball C decreases over α=0.3 at N=3000 rpm. From this result, when a ball is struck by a bat and rotates at a high speed of rotation, the drag of the rubber ball decreases beyond that of a hard ball. From the viewpoint of aerodynamics, it can be concluded that a rubber ball will fly farther than a traditional hard ball.

Next, the change of C_L is compared. As shown in Fig. 10, the smooth test ball generated negative lift at Re=1.2×10^5 and 1.6×10^5. Although the C_L of the smooth test ball is fixed at -0.25 to -0.2, even if the spin rate changes, the C_L of test balls A~E increases as α increases, as shown in Fig. 13. It is considered that since the influence by the surface structure becomes large as α increase, so the lift

increases. When the Reynolds number is Re=1.6×10^5, the C_L of test balls A~E increase linearly as a increases. At Re=1.6×10^5 the test balls without rotation have reached the supercritical region. So, the flow around test balls becomes stable and the values of C_L exhibit a linear relation.

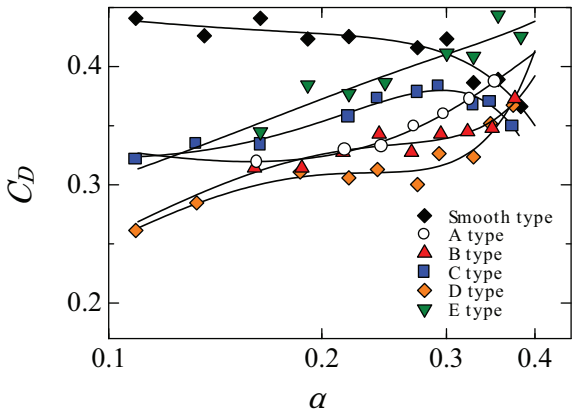

Fig. 12. Drag coefficient vs. spin rate (Re=1.6×10^5).

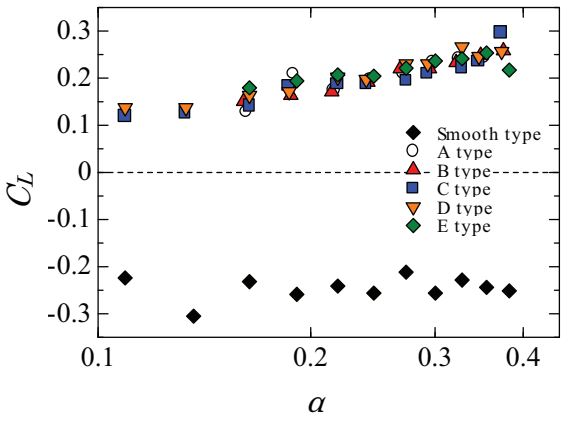

Fig. 13. Lift coefficient vs. spin rate (Re=1.6×10^5).

4. Conclusion

The aerodynamic characteristics, such as the lift and drag, of official rubber baseballs are examined experimentally by comparing the characteristics of a smooth surface ball and rubber balls having different surface structures. From the analysis of the experimental results, the following conclusions have been obtained.

(1) The dimpled rubber ball has a critical region where the drag coefficient decreases in the same way as that for the smooth ball.
(2) Depending on the surface structure of test ball, the aerodynamic characteristics differ significantly. When dimples are added to the balls with seams, the critical region moves toward the lower Reynolds number side, but the minimum drag coefficient increases.
(3) In the critical region, the drag coefficient varies depending on the rotating angle of the ball.
(4) The flow patterns for a smooth ball having different surface structures and the flow mechanism around a sphere have been clarified.
(5) In the case of the smooth ball, when the Reynolds number is Re=1.2×10^5 and 1.6×10^5, the lift occurred in the negative direction in a=0.1~0.6. Moreover, the lift has shifted in the positive direction for a>0.6.
(6) For the rubber ball and the traditional hard ball, without rotation, the values for C_D are almost same. However, when rotating, the C_D of the rubber ball is lower than that of the hard ball.
(7) The values of C_D differ depending for test balls A~E and increase as a increases. The values of C_L increase linearly as a increases.

References

Mizota, T., Kuba, H. and Okajima, A., Erratic Behavior of Forkball, J. of Wind Engineering 62(1995), 3-21.

Bearman, P. W. and Harvey, J. K., Golf Ball Aerodynamics, Aeronautical Quarterly, 27(1976), 112-122.

Taneda, S., Negative Magnus Effect, Reports of Research Institute for Applied Mechanics, (1957).

Author Profile

Katsumi Aoki: He received his M.Sc.(Eng.) and Ph.D. in mechanical engineering from Tokai University in 1967 and 1986. He received his degree in mechanical engineering and his from Tokai University. After obtaining his M.Sc. he worked as a research assistant, a lecturer, and an associate professor at Tokai University before taking up his current position as a professor of Tokai University. His current research interests cover flow around a rotating circular cylinder with and without grooves, flow around a rotating sphere, possibility of drag reduction using triangular cavities, and flow visualization of complicated flow fields, as in the centrifugal blower, by the spark tracing method.

Yasuhiro Kinoshita: He received his B. Eng. and M. Eng. Degree in mechanical engineering from Tokai University in 2000 and 2002. Since 2002, he is currentry an engineer at NORITAKE Co., LIMITED. His research interest is the aerodynamic characteristics of baseballs.

Jiro Nagase: He received his B.Ec. degree in Economics from Meiji University in 1957. His research interests are the flying characteristics of rubber balls used in baseball games and other sports balls. He is President of Nagase Kenko Co., which manufactures sporting goods in Japan. He is the Chairman of the Rubber Ball Industrial Club, Director of the International Exchange Association on rubber balls for junior baseball and Trustee of the World Children's Baseball Foundation

Yasuki Nakayama: He received his B.Sc.(Eng) degree in Mechanical Engineering in 1952 and his Ph.D. in Mechanical Engineering in 1963 from Waseda University. He joined the National Railway Technical Research Institute and conducted several studies in the area of fluid mechanics. After leaving NRRI, as a Professor of Tokai University, he has been responsible for education and research on fluid mechanics and visualization. At present, he is serving concurrently as President of the Future Technology Research Institute.
He has received a Medal with a Purple Ribbon from the Emperor of Japan, and many distinctions and awards for his outstanding research. He was a Visiting Professor of Southampton University, UK, President of The Visualization Society of Japan. He has published 10 books and more than 180 research papers.